

Energy Partitioning and Evapotranspiration over a Rice Paddy in Southern Brazil

ANDREA UCKER TIMM,* DÉBORA R. ROBERTI,⁺ NEREU AUGUSTO STRECK,[#]
 LUIS GUSTAVO G. DE GONÇALVES,[@] OTÁVIO COSTA ACEVEDO,⁺ OSVALDO L. L. MORAES,[@]
 VIRNEI S. MOREIRA,[&] GERVÁSIO ANNES DEGRAZIA,⁺ MITJA FERLAN,^{**} AND DAVID L. TOLL⁺⁺

** Faculdade da Serra Gaúcha, Caxias do Sul, Rio Grande do Sul, Brazil*

⁺ Departamento de Física, Universidade Federal de Santa Maria, Santa Maria, Rio Grande do Sul, Brazil

[#] Departamento de Fitotecnia, Universidade Federal de Santa Maria, Santa Maria, Rio Grande do Sul, Brazil

[@] Centro de Previsão de Tempo e Estudos Climáticos, Instituto Nacional de Pesquisas Espaciais, Cachoeira Paulista, São Paulo, Brazil

[&] Universidade Federal do Pampa, Campus Itaqui, Itaqui, Rio Grande do Sul, Brazil

*^{**} Slovenian Forestry Institute, Ljubljana, Slovenia*

⁺⁺ Hydrological Sciences Laboratory, NASA Goddard Space Flight Center, Greenbelt, Maryland

(Manuscript received 7 August 2013, in final form 21 March 2014)

ABSTRACT

During approximately 80% of its growing season, lowland flooded irrigated rice ecosystems in southern Brazil are kept within a 5–10-cm water layer. These anaerobic conditions have an influence on the partitioning of the energy and water balance components. Furthermore, this cropping system differs substantially from any other upland nonirrigated or irrigated crop ecosystems. In this study, daily, seasonal, and annual dynamics of the energy and water balance components were analyzed over a paddy rice farm in a subtropical location in southern Brazil using eddy covariance measurements. In this region, rice is grown once a year in low wetlands while the ground is kept fallow during the remaining of the year. Results show that the energy budget residual corresponded to up to 20% of the net radiation during the rice-growing season and around 10% for the remainder of the year (fallow). The energy and water balance analysis also showed that because of the high water table in the region, soil was near saturation most of the time, and latent heat flux dominated over sensible heat flux by up to one order of magnitude in some cases. The estimate of evapotranspiration ET using the crop coefficient multiplied by the reference evapotranspiration $K_c ET_o$ and the Penman–Monteith equation ET_{PM} , describing the canopy resistance through leaf area index (LAI) obtained by remote sensing, represent well the measured evapotranspiration, mainly in the fallow periods. Therefore, using a specific crop parameter like LAI and crop height can be an easy and interesting alternative to estimate ET in vegetated lowland areas.

1. Introduction

Rice (*Oryza sativa* L.) constitutes the staple food for about half of the world's population. About 150 million ha of land are annually planted with rice worldwide, with a total production of about 590 million tons. Nearly 75% of the rice production comes from flooded irrigated rice paddies. Brazil is among the top 10 rice-producing countries and is the largest outside Asia, producing about 12 million tons of rice annually over 2.4 million ha of land (Conab 2013).

In Brazil, 60% of the rice is produced in the lowlands of the Rio Grande do Sul state and comprises an area of approximately 1 million ha. This subtropical climate region is located in the southernmost portion of the country (30°–32°S, 51°–57°W). A typical agronomic timeline consists of the following steps: 1) conventional preparation by tilling the dry soil (dry tillage) for good seedbed preparation during austral spring (October–November); 2) “dry” (aerobic) soil sowing during November; and 3) flood irrigation keeping a 5–10-cm water layer above soil surface, starting at the onset of tilling (about 30 days after sowing) until 15 days before harvest in early austral fall (March–April). Therefore, most of the growing season (which comprises 80% of the total time), takes place under anaerobic water-saturated soil conditions (Streck et al. 2011). From April to October, the lowland areas are kept fallow, the soil is water saturated

Corresponding author address: Débora R. Roberti, Physics Department, Federal University of Santa Maria, Av. Roraima, n. 1000, Santa Maria, Rio Grande do Sul 97105900, Brazil.
 E-mail: debora@ufsm.br

(anaerobic) most of the time, and crop residue is either incorporated into the soil (tillage) or kept as mulch (no tillage). Such a rice production timeline differs from the practice in Asia, where rice is produced during two growing seasons along one calendar year (Tsai et al. 2007; Alberto et al. 2011).

A lowland flooded irrigated rice ecosystem differs greatly from any other upland nonirrigated or irrigated crop ecosystem because of the continuous water layer above the soil surface, which strongly affects the surface energy balance components (Tsai et al. 2007; Maruyama and Kuwagata 2010; Alberto et al. 2011; Hatala et al. 2012; Hosson et al. 2012). Furthermore, rice paddies are usually part of a larger area of lowlands within a river basin, creating a microclimate with large water availability for evapotranspiration ET, which in turn increases the atmospheric specific humidity near the surface. Therefore, understanding and describing the energy partitioning variability over flooded rice paddies is essential for a good performance of surface–atmosphere interaction models in lowlands, especially considering that agricultural irrigated areas are usually not represented well in such models (Noilhan and Planton 1989; Foley et al. 1996; Walko et al. 2000; Ek et al. 2003).

Evapotranspiration is also important for a better understanding of the hydrological and biogeochemical cycles as well as the surface energy balance in agricultural and other ecosystems. Moreover, evapotranspiration is typically the largest component of the water balance in agricultural areas (Suyker and Verma 2008) as well as a great consumer of available solar energy, especially in irrigated agricultural areas, consuming 60%–80% of the net radiation during crop-growing seasons (Wilson and Baldocchi 2000).

Being a major component of the water consumption in rice paddies, an accurate estimate of ET is important for several purposes. One of them is to improve the efficiency of water resources management and irrigation requirements in irrigated rice fields where water consumption may be 2–3 times greater than in other crops growing in uplands (Vu et al. 2005). The majority of rice evapotranspiration studies have been conducted over regions with two annual growing seasons (Alberto et al. 2011; Hosson et al. 2012). Consequently, the ET contribution, during the fallow period, to the annual evapotranspiration and its annual variability in subtropical regions with only one annual rice-growing season has not been fully addressed. Such lack of knowledge becomes critical in rice-based agroecosystems with a long fallow period, for example, southern Brazil. Recent studies have shown the important role of the nongrowing season or fallow periods to the energy flow (Kucharik and Twine 2007). Nonetheless, more efforts need to be devoted to

fully understand the dynamics of the energy balance components on an annual basis, especially in flooded rice ecosystems.

Accordingly, a discussion regarding year-round energy eddy covariance flux measurements in a flooded rice paddy in southern Brazil is presented in this work with the following goals: 1) to quantify the seasonal and annual distribution of the energy balance components; 2) to examine how environmental variables influence the seasonal distribution of these fluxes; 3) to evaluate the growing season and fallow periods' contribution to the annual ET totals and to quantify the variation of crop coefficient K_c throughout the growing season; and 4) to evaluate the performance of the Penman–Monteith equation, based on surface factors over rice crops in lowland areas.

2. Materials and methods

a. Site description

Field measurements were taken over a 50 ha farm with flooded irrigated rice in southern Brazil. The experimental site is located in the vicinity of the city of Paraíso do Sul (29°44'39.6"S, 53°8'59.8"W; 108 m), in the state of Rio Grande do Sul, Brazil. The site is part of a broader lowland area, which has been cultivated with irrigated rice since the early 1980s (Fig. 1). The local climate is humid subtropical, like the majority of rice zones in the state. Furthermore, most of the freshwater used for the rice fields' irrigation in this region comes from small creeks and artificial reservoirs.

The study period is from 22 July 2003 to 21 July 2004, whereby rice was sown on 25 November 2003 and harvested on 4 April 2004. During the fallow period, the surface remained covered with just short vegetation composed by wild grasses and other weedy plants, for example, *Heterenthera reniformis*, *Echinochloa crusgalli*, *Brachiaria plantaginea*, *Digitaria* sp., and *Luziola peruviana*. From late December through mid-March, soil was kept flooded with approximately 10-cm water depth. The rice cultivar grown during the 2003/04 season was IRGA 417, a modern, well-adapted, and widely grown rice cultivar in Rio Grande do Sul.

The soil type at the experimental site is Humic Planosols [Food and Agriculture Organization (FAO)] or Typic Albaqualf (Soil Survey Staff 1999), a typical flooded soil where rice is grown in Rio Grande do Sul. Furthermore, the particle-size distribution and some other physical properties in the upper 1-m layers of the soil are listed in Table 1. It is noteworthy that the permanent wilting point for all soil layers is lower than the measured soil water availability. Nevertheless, the top



FIG. 1. Paraíso do Sul experiment site located in southern South America. The delimited area represents the rice paddy cultivation and the fetch of the flux tower. The figure was not obtained in the period of the experiment analyzed in this study.

layers become more vulnerable to saturation because of smaller soil field capacity values when compared to the deeper layers.

b. Eddy covariance and meteorological data

Sensible and latent heat fluxes were measured using eddy covariance techniques. From high-frequency wind speed, temperature, and humidity measurements, the vertical fluxes of a given scalar are given by the covariance between fluctuations of vertical wind velocity and of the respective scalar. The sensor set includes a 3D sonic anemometer (CSAT3; Campbell Scientific Inc., Logan, Utah) for turbulent wind component measurements and an infrared open-path gas analyzer (LI-7500; LI-COR Inc., Lincoln, Nebraska) to measure H_2O concentrations, at 10-m height and sampled at a 16-Hz frequency. Additionally, sensors for temperature and relative humidity (HMP45C-L; Campbell Scientific Inc., Logan, Utah), pressure (CS105; Vaisala, Vantaa, Finland), precipitation (TB4 Rain Gauge; Campbell Scientific Inc., Logan, Utah), and net radiation (NR LITE; Kipp & Zonen, Delft, The Netherlands)

were installed at 10-m height for 1-Hz atmospheric measurements.

Soil parameters were also collected at 1 Hz, including soil moisture at 0.2-m depth (PR1; Delta-T Devices, Cambridge, United Kingdom); soil temperature at 2-, 5-, and 10-cm depths (STP01; Hukseflux Thermal Sensors, Delft, The Netherlands); and ground heat flux at 7 cm (HFP01SC-L; Hukseflux Thermal Sensors, Delft, The Netherlands). Further details including instrument errors, measurements uncertainties, and site characteristics can be found in [Acevedo et al. \(2006, 2009\)](#).

Soil heat flux G has been estimated through the sum of ground heat flux F_g and the soil and water heat storage ΔG . Because of the lack of water temperature measurements, the temperature variation at 2-cm depth was used to compute water heat storage. Thus, soil and water heat storage were estimated as follows:

$$\Delta G = \frac{c_s \Delta T_s dz_s}{dt} + \frac{c_a \Delta T_a dz_a}{dt}, \quad (1)$$

where c_s is the volumetric soil heat capacity and c_a is the volumetric water heat capacity ($4.186 \text{ MJ m}^{-3} \text{ } ^\circ\text{C}^{-1}$);

TABLE 1. Physical properties of the soil at the experimental site in the paddy rice in Paraíso do Sul, Brazil.

Depth (cm)	Sand (%)	Clay (%)	Silt (%)	Field capacity (%)	Permanent wilting point (%)	Water available (%)	Macroporosity (%)	Microporosity (%)
10	23.70	14.90	61.40	0.37	0.14	0.22	0.08	0.39
20	20.30	16.50	63.20	0.35	0.17	0.18	0.04	0.36
30	14.05	13.40	72.55	0.38	0.19	0.19	0.03	0.39
40	11.70	20.30	68.00	0.40	0.14	0.26	0.02	0.41
60	30.05	16.80	53.15	0.39	0.16	0.24	0.05	0.40
100	23.25	26.60	50.15	0.54	0.18	0.36	0.07	0.58

ΔT_5 and ΔT_2 represent the soil temperature variation at 5- and 2-cm depths, respectively; dt is the time step ($dt = 3600$ s); dz_s is the soil layer above the soil temperature sensor; and dz_a is the depth of the water layer. The second term in Eq. (1) appears during the soil flooding (i.e., when soil moisture at 0.2 cm exceeds $0.5 \text{ m}^3 \text{ m}^{-3}$). A sensitivity analysis using saturated clay and sandy soil following Oke (1987) was firstly performed in order to estimate c_s . Nevertheless, the differences between the annual averaged soil and water heat storage were on the order of 10^{-4} W m^{-2} . Consequently, the mean value of saturated clay and sandy soil ($3.03 \text{ MJ m}^{-3} \text{ }^\circ\text{C}^{-1}$) suggested by Alberto et al. (2011) was adopted for this study.

c. Eddy covariance data processing, gap filling, and energy balance

Before computing the turbulent fluxes, the raw data undergo a quality-control stage (Baldocchi et al. 1988; Wyngaard 1990; Aubinet et al. 2000), which comprises inadequate sensor frequency response correction, despiking, coordinate rotation, and air density adjustments.

The turbulent fluxes were calculated over 1-h windows, allowing low-frequency processes, which in turn represent a relevant contribution to the energy budget closure (Sakai et al. 2001; Cava et al. 2008). Moreover, periods that contained physically inconsistent data (i.e., latent heat flux LE values < -50 or $> 1000 \text{ W m}^{-2}$, sensible heat flux H values < -200 or $> 1000 \text{ W m}^{-2}$) were discarded. Including missing data due to instrument malfunction, the total gap in the data, after applying the quality-control procedure, was approximately 22%. Nonetheless, this data gap is relatively low when compared to other eddy covariance measurements (Alberto et al. 2011), consequently resulting in a high-quality dataset. Data gaps shorter than 2 h were filled using a simple interpolation method, whereas in data gaps longer than 2 h, LE and H were estimated as a function of the available energy. For the latter, linear regression between hourly values of LE or H and available energy ($R_n - G$; where R_n is the net radiation flux density at the crop surface) was computed using 15-day moving windows before filling in the missing flux data. This regression slope also gives an estimate of the energy balance closure.

The energy balance closure was calculated for three distinct periods: Fallow 1, comprising 126 days from 22 July to 24 November 2003 (austral winter/spring); Rice, comprising 132 days (i.e., from sowing to harvest) from 25 November 2003 to 4 April 2004 (austral spring/summer); and Fallow 2, comprising 108 days from 5 April to 21 July 2004 (austral autumn/winter).

The residual available energy RAE calculated using the energy balance available components (Hernandez-Ramirez et al. 2010),

$$\text{RAE} = R_n - G - H - \text{LE}, \quad (2)$$

was used to correct H and LE in order to close the energy balance. Furthermore, the percentage of RAE to be distributed between H and LE was computed through the use of the Bowen ratio.

To obtain the measured daily ET, the corrected LE ($\text{MJ m}^{-2} \text{ day}^{-1}$) was used in the equation

$$\text{ET} = 10^{-9} \left(\frac{\text{LE}}{\rho_a \lambda} \right), \quad (3)$$

where λ is the latent heat for vaporization ($2.45 \times 10^6 \text{ J Kg}^{-1}$) and ρ_a is the air density (998.21 Kg m^{-3}), both at the standard temperature (20°C). In Eq. (3), ET is in units of millimeters per day. Daily ET values were accumulated to obtain seasonal values.

d. The evapotranspiration using Penman–Monteith equation

The Penman–Monteith equation combines aerodynamic and thermodynamic aspects, including the resistance to the sensible heat and atmospheric water vapor, and surface resistance to estimate the flow of water vapor between the surface and the atmosphere. The estimated evapotranspiration using the Penman–Monteith equation (hereafter named ET_{PM}) is defined as

$$\text{ET}_{\text{PM}} = \left\{ \frac{\Delta(R_n - G) + \rho_a c_p \frac{(e_s - e_a)}{r_a}}{\left[\Delta + \gamma \left(1 + \frac{r_s}{r_a} \right) \right]} \right\} \frac{1000}{\lambda \rho_w}, \quad (4)$$

where R_n is the net radiation flux density at the crop surface (W m^{-2}), G is the soil heat flux density (W m^{-2}), ρ_a is the mean air density at constant pressure (kg m^{-3}), c_p is the specific heat of air ($\text{J kg}^{-1} \text{ K}^{-1}$), e_s is the saturation vapor pressure (kPa), e_a is the actual vapor pressure (kPa), $(e_s - e_a)$ is the saturation vapor pressure deficit (kPa), Δ is the slope of the vapor pressure curve ($\text{kPa } ^\circ\text{C}^{-1}$), γ is the psychrometric constant ($\text{kPa } ^\circ\text{C}^{-1}$), r_s is the bulk surface resistance (s m^{-1}), r_a is the aerodynamic resistance (s m^{-1}), λ is the vaporization of latent heat (J kg^{-1}), and ρ_w is the water density (kg m^{-3}). Equation (4) thus yields the evapotranspiration (mm s^{-1}) and the daily integration (mm day^{-1}). The aerodynamic resistance can be defined as

$$r_a = \frac{\ln \left(\frac{z - d}{z_{0m}} \right) \ln \left(\frac{z - d}{z_{0h}} \right)}{k^2 u_z}, \quad (5)$$

where z is the height at which wind speed is measured, d is the displacement height, z_{0m} is the roughness height

for momentum, z_{0h} is the roughness height for water vapor, $k = 0.4$ is the von Kármán constant, u_z is the horizontal wind speed at the sensor height z , and z_v is the vegetation height. The definitions for d , z_{0m} , and z_{0h} are, respectively,

$$d = \frac{2}{3}z_v, \quad (6)$$

$$z_{0m} = 0.1z_v, \quad \text{and} \quad (7)$$

$$z_{0h} = 0.1z_{0m}. \quad (8)$$

The surface or canopy resistance can be written as

$$r_s = \frac{r_l}{\text{LAI}}, \quad (9)$$

where r_l is the stomatal resistance and LAI is the leaf area index. In Eq. (4), LAI and z_v represent the surface effects.

In this study, LAI was obtained by remote sensing from the Moderate Resolution Imaging Spectroradiometer (MODIS) Collection 5 (MOD15A2) global products. The product is composed every 8 days at 1-km resolution on an integerized sinusoidal (IS) 10° grid. Daily values for LAI were calculated from a simple linear interpolation method. Although z_v was not measured in the experiment, it was estimated as a linear function from sowing until the maximum LAI. We assumed a maximum $z_v = 0.8$ m in the rice-growing season, and in the fallow periods we set $z_v = 0.1$ m to represent a plowed land or the spontaneous vegetation.

e. The FAO reference Penman–Monteith equation and crop coefficient

Reference evapotranspiration ET_o multiplied by K_c is one of the most widely used approaches for calculating ET and water consumption in irrigated crops (de Medeiros et al. 2005). According to Grismer et al. (2002), about 50 methods are available for estimating ET_o , often generating inconsistent results. The FAO Penman–Monteith method has been used as a standard method for calculating ET_o from meteorological data because it incorporates both physiological and aerodynamic parameters (Allen et al. 1998; de Medeiros et al. 2005; Vu et al. 2005). The method was published in FAO Irrigation and Drainage Paper 56 (FAO-56). Nevertheless, a few studies have evaluated the FAO-56 method for estimation of evapotranspiration and for evaluation of crop coefficient for rice fields (Shah and Edling 2000; Tyagi et al. 2000; Bethune et al. 2001; Lage et al. 2003; Lecina et al. 2003; Alberto et al. 2011).

The reference evapotranspiration rate, calculated using Eq. (4), from a hypothetical reference crop, 12 cm

tall, canopy resistance of 70 s m^{-1} , and albedo of 0.23, is similar to the evapotranspiration from a large grass area. To estimate the canopy resistance [Eq. (9)], this method uses an active LAI, that is, just the upper half of dense clipped grass is actively contributing to the surface heat and vapor transfer. The FAO Penman–Monteith equation for calculating daily ET_o (mm day^{-1}) using average daily data (24-h time step) is (Allen et al. 1998):

$$ET_o = \frac{0.408\Delta(R_n - G) + \gamma(900/T + 273)U_2(e_s - e_a)}{\Delta + \gamma(1 + 0.34U_2)}, \quad (10)$$

where T is the air temperature at 2-m height ($^{\circ}\text{C}$) and U_2 is the wind speed at 2-m height (m s^{-1}). In this study, the wind speed at 2-m height was calculated from the measured wind speed at 10-m height. The velocity profile is affected by several factors, including surface and vegetation type, which are difficult to estimate. Allen et al. (1998) suggested the logarithmic profile of wind speed as

$$U_z = \frac{4.87U_z}{\ln(67.8z - 5.42)}, \quad (11)$$

where z is the height above the surface and U_z is the observed wind speed.

Daily values of K_c were calculated from the ratio of measured ET [Eq. (3)] and ET_o [Eq. (10)] during the rice-growing season (from sowing to harvest):

$$K_c = \frac{ET}{ET_o}. \quad (12)$$

3. Results and discussion

a. Environmental conditions

Daily variation of the meteorological variables throughout the year (from 22 July 2003 to 21 July 2004) at the study site are shown in Fig. 2. The highest air temperature values occurred from January to mid-February (Fig. 2a), with mean daily values around 27°C , whereas the lowest values occurred during July (about 7°C). During the rice-growing season (from 25 November 2003 to 4 April 2004), the temperature variation was not large, favoring crop growth and development. The vapor pressure deficit (VPD) followed the variation of air temperature, and the values were less than 1 kPa in most of days, characterizing an atmosphere with low water demand for plant transpiration or soil evaporation (Kiniry et al. 1998). Relative humidity, as expected, showed an opposite pattern (Fig. 2b) varying from 54.4% to 98.1% on a daily-average basis, often between 65% and 93%.

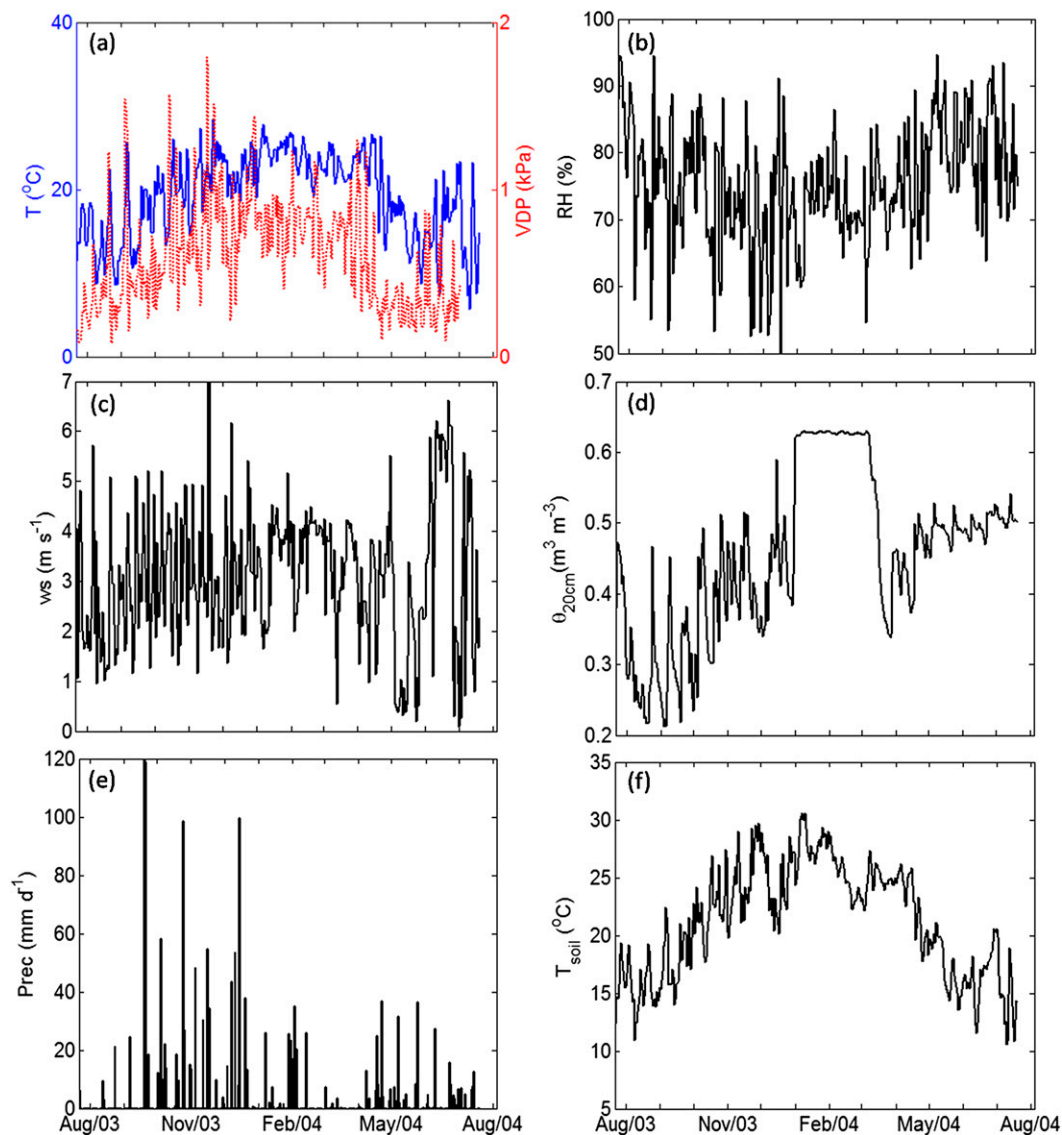


FIG. 2. Daily values of weather variables during the study period from 22 Jul 2003 to 21 Jul 2004 in Paraíso do Sul, Brazil: (a) mean air temperature and VPD, (b) relative humidity, (c) wind speed, (d) volumetric soil water content at 20-cm depth, (e) precipitation, and (f) soil temperature at 2-cm depth.

Daily-averaged wind speed (Fig. 2c) reached 6.0 m s^{-1} , with an average value near 3.0 m s^{-1} .

The 20-cm soil water content varied from 0.3 to $0.6 \text{ m}^3 \text{ m}^{-3}$, with constant maximum values from early January to late March, during the flooded period in the growing season (Fig. 2d). Precipitation was generally well distributed throughout the year (Fig. 2e), although accumulated precipitation from October to December corresponded to 40% of the total rainfall. The total precipitation during the 366 days was 1630 mm, and during the 134-day-long growing season the rainfall summed 477 mm. The two days with the most intense precipitation

occurred 20 and 21 September 2003 (122 and 119 mm, respectively).

The highest soil temperature values for the top 2-cm layer occurred between January and February, with average daily values around 28°C (Fig. 2f). However, in this period, the daily cycle did not show as large a variation as the other periods (data not shown), which is associated with the greater water heat capacity that maintains the soil warmth. The values for the deeper layers (5- and 10-cm depth) were not shown here because the daily average does not differ substantially for these layers.

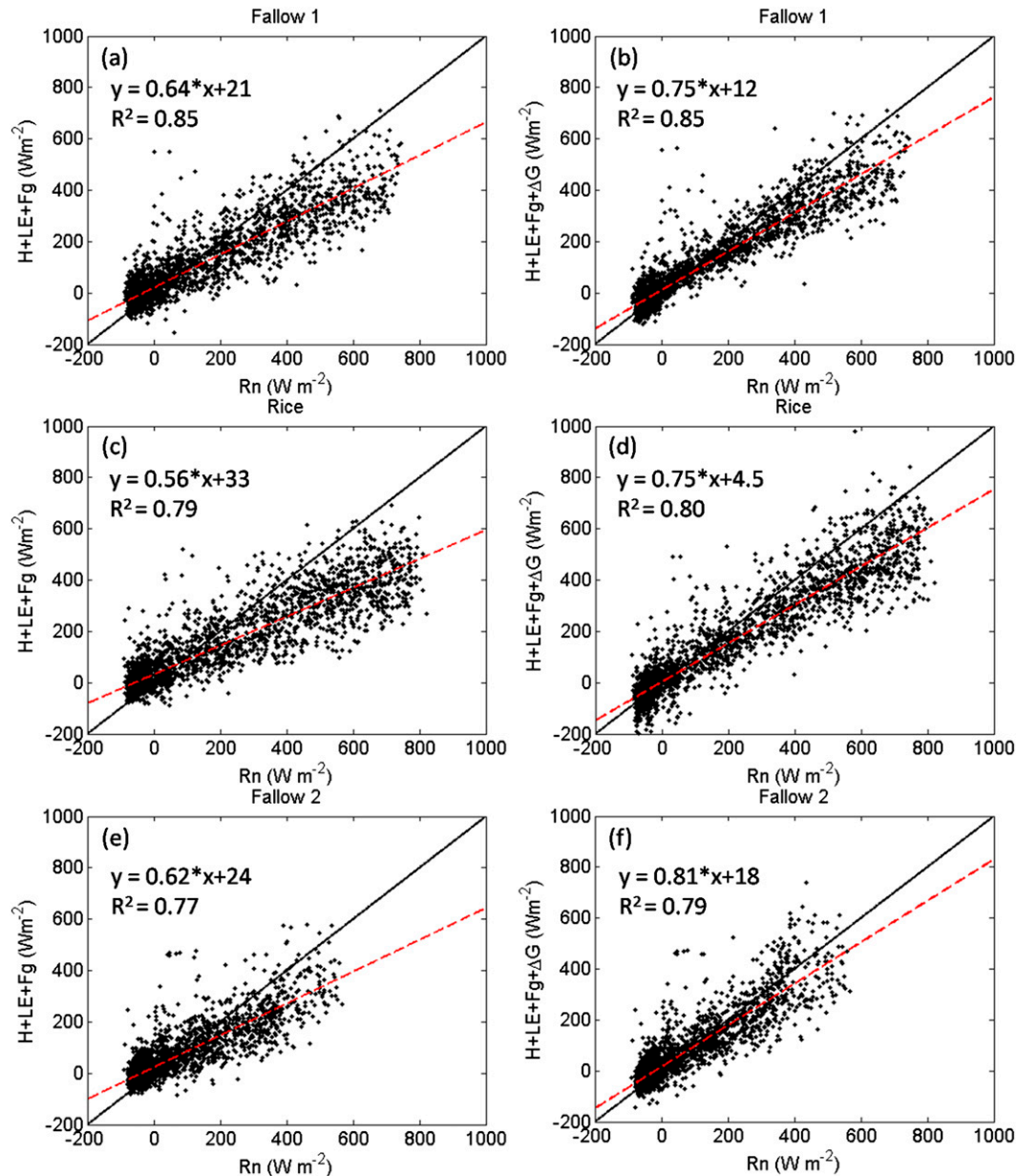


FIG. 3. Scatterplots of the half-hour energy balance closure: R_n vs the sum of H and LE soil heat fluxes computed for (a), (b) Fallow 1; (c), (d) Rice; and (e), (f) Fallow 2 in a rice paddy in Paraíso do Sul, Brazil. The soil heat flux was estimated using F_g (left) or the sum of F_g and ΔG (right). Dashed red line represents the linear fit of the data. For reference, the 1:1 line is also shown (solid black line).

In this flooded rice paddy, the environmental conditions, especially VPD, are similar to those reported by Alberto et al. (2009), who compared a flooded rice field to an aerobic field in the Philippines. They concluded that the former had significantly lower VPD than the latter, from tilling to flowering. The permanent water depth above soil surface plays an important role in the moisture supply to the near-surface atmosphere during the rice-growing season.

b. Energy partitioning

The effect of the soil and water heat storage on the hourly energy balance closure was examined by comparison of the slope of the linear fit between net radiation (i.e., R_n) and the energy budget components (H , LE , F_g , and ΔG ; Fig. 3). When ΔG was not included, the slope of the linear regression was 0.64, 0.56, and 0.62, with R^2 of 0.85, 0.79, and 0.77, for Fallow 1, Rice, and

TABLE 2. Daily values of energy balance components for the three periods (Fallow 1, Rice, and Fallow 2) on a rice paddy area in Paraiso do Sul, Brazil.

	Fallow 1 (126 days)	Rice (132 days)	Fallow 2 (108 days)
R_n ($\text{MJ m}^{-2} \text{ day}^{-1}$)	7.79	12.54	3.89
LE ($\text{MJ m}^{-2} \text{ day}^{-1}$)	5.34	7.97	3.68
H ($\text{MJ m}^{-2} \text{ day}^{-1}$)	1.23	1.47	1.22
G ($\text{MJ m}^{-2} \text{ day}^{-1}$)	0.28	0.39	0.37
ΔG ($\text{MJ m}^{-2} \text{ day}^{-1}$)	0.05	-0.02	0.29
RAE ($\text{MJ m}^{-2} \text{ day}^{-1}$)	0.90	2.73	-0.94
LE/ R_n	0.69	0.64	0.94
H/ R_n	0.16	0.12	0.31

Fallow 2, respectively, indicating that in none of the periods is the net radiation accounted for by the total energy fluxes measured (Figs. 3a,c,e). When the storage term [Eq. (1)] is included in the energy balance closure, the slope was 0.75, 0.75, and 0.81 with R^2 of 0.85, 0.80, and 0.79, for Fallow 1, Rice, and Fallow 2, respectively (Figs. 3b,d,f). For the entire period, the slope was 0.75 (data not shown), the same coefficient reported by Hossen et al. (2012) for a rice paddy. Also in a rice paddy study, Hatala et al. (2012) found 0.65 as a slope for hourly energy balance closure. These authors suggest that the lower energy balance closure at the rice paddy is due to the rough approximation of the heat storage in the water column, as the change in water temperature was measured solely at a single depth in the water column. In our case, we estimate the storage energy in water using the temperature in the upper soil layer (2-cm depth). However, it is difficult to make accurate measurements of ΔG when soil heat capacity varies with depth because of variation in soil moisture and/or of large spatial and temporal variability in soil heat fluxes across a measurement site (Leuning et al. 2012). Several experimental and numerical studies found a surface imbalance ranging from about 10% to 30%, typically related to an underestimation of surface energy fluxes measured by the eddy covariance technique at a single measurement point (Tsvang et al. 1991; Kanemasu et al. 1992; Aubinet et al. 2000; Wilson et al. 2002; Kanda et al. 2004).

Table 2 shows the daily values of the energy balance components and energy partitioning (LE/ R_n and H/ R_n) during Fallow 1, Rice, and Fallow 2. Net radiation was mostly explained by LE, representing 69% of R_n during Fallow 1, 64% during Rice, and almost 100% during Fallow 2. Latent heat flux was nearly 80% greater than sensible heat flux during Fallow 1 and Rice periods and 65% greater during Fallow 2. These results suggest that there is large water availability for evapotranspiration during the fallow periods in this region and as well as the low VPD throughout the entire year (Fig. 2a). The

magnitude of R_n and LE was significantly different during the three periods, whereas H and F_g remained nearly constant, although F_g was negative in Fallow 2, suggesting that soil surface warming occurred. The soil and water heat storage between the surface and the flux plate was almost zero during Fallow 1 and Rice periods and on the same order of magnitude as of the ground heat flux, albeit with the opposite sign in Fallow 2. Thus, the energy transferred from the subsoil during Fallow 2 was almost entirely used for heating the surface layer. The RAE resulting from the energy balance closure was $0.90 \text{ MJ m}^{-2} \text{ day}^{-1}$ (representing 10% of R_n) during Fallow 1 and 31.54 W m^{-2} (representing 20% of R_n) during the Rice period, and during Fallow 2 the residual was below zero, that is, $-0.94 \text{ MJ m}^{-2} \text{ day}^{-1}$ (representing -20% of R_n). These results suggest that the soil was the main source of energy to the atmosphere during Fallow 2, which is reasonable as this period was during austral fall and winter.

Figure 4 shows the mean daily cycle of the energy budget components (R_n , LE, H , F_g , and ΔG) for the three periods. During Fallow 1, the soil had a reduced vegetation cover, so that most of the solar radiation reached the wet surface. Consequently, F_g and H had similar daily cycles, whereas ΔG represents a greater soil warming in the morning and cooling in the afternoon. During the Rice period, as the plant canopy covers the soil surface, intercepting solar radiation, less energy is available in the soil surface. Furthermore, as the rice paddy remains irrigated during most of the period, the saturated soil and the water layer above the soil surface are additional reducing factors for the soil heating, therefore contributing to delaying the daily F_g cycle. In this period, ΔG is considered as the sum of the energy stored above the flux plate and the energy stored in the water layer. Notwithstanding the daily average in this period is close to zero (Table 2), there is a greater increase in the magnitude of ΔG during the morning and decrease during the afternoon, when compared with Fallow 1. During Fallow 2 (Fig. 4e), the postharvesting straw left on the ground combined with the austral fall/winter low temperatures contributed to the high soil moisture accumulation (see Fig. 2d) when compared to Fallow 1. Such high soil moisture contributes to the shift of the maximum F_g from midday (Fallow 1) to mid-afternoon (similar to the Rice period). The shifting in the peak of F_g occurs because of the high water heat capacity, which delays the energy transport from surface toward deeper soil layers. Moreover, H is greater than F_g throughout most of the daily cycle, except toward the end of the afternoon (Fig. 4e). Because of high soil water availability during all periods, most of the available energy was partitioned into LE, reaching 300 W m^{-2} at

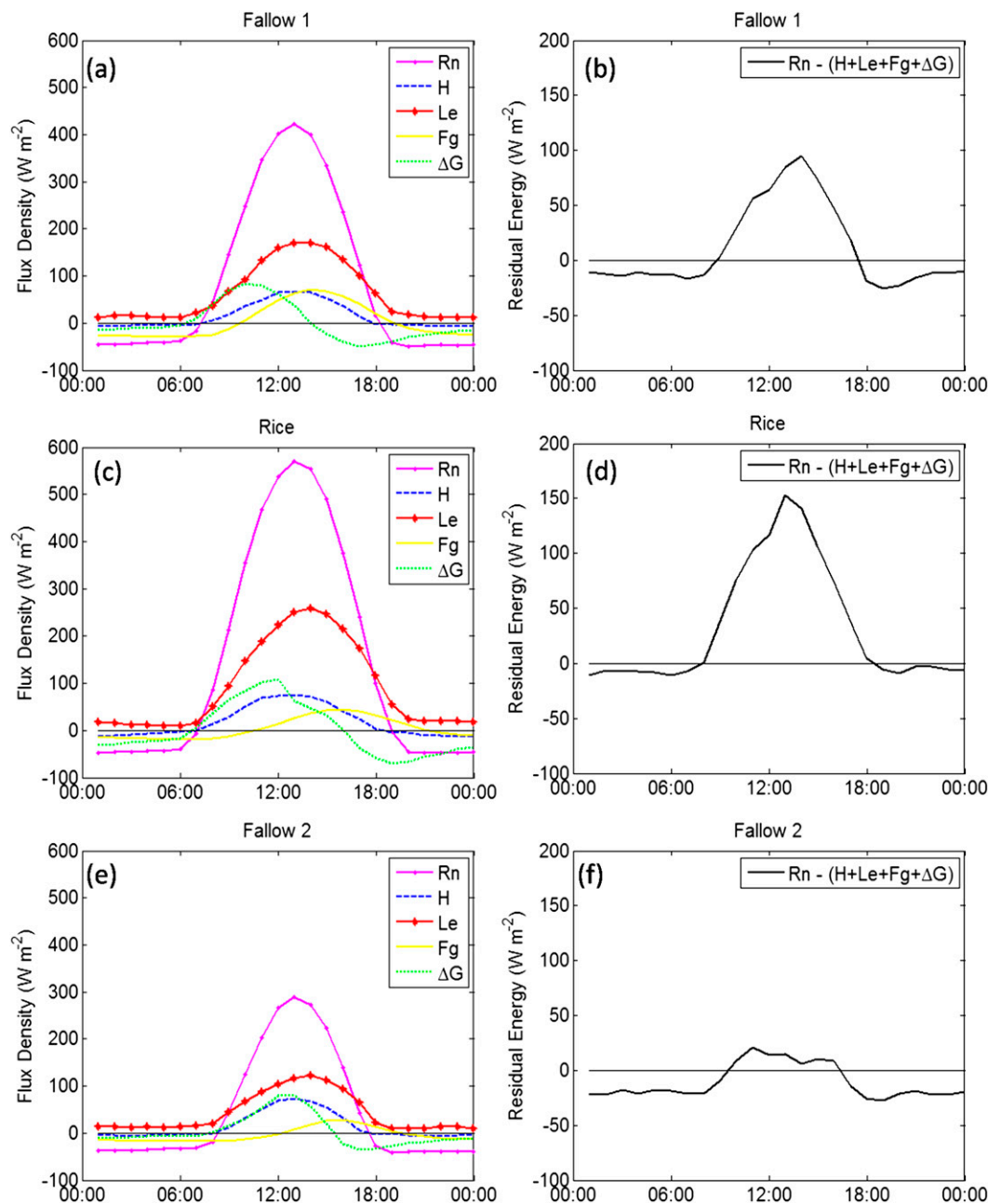


FIG. 4. Mean daily cycle of the components of (left) energy balance and (right) RAE computed for the (a),(b) Fallow 1; (c),(d) Rice; and (e),(f) Fallow 2 periods in a rice paddy in Paraíso do Sul, Brazil.

noon during the Rice period. On average, the Rice period presented 40% more LE than the fallow periods.

The daily pattern of residual energy is consistent in all three periods (Figs. 4b,d,f), with energy missing during daytime and a surplus of energy with respect to net radiation at nighttime, similar to the patterns found by Cava et al. (2008). During the Rice period, daytime residual energy is larger in magnitude than during both Fallow periods, partially because of the energy stored

within the canopy that is not accounted for by the measurement instruments. That is to say, part of the energy that enters the system is not computed in the energy balance equation.

The Bowen ratio ($\beta = H/LE$) calculated from daily-mean sensible and latent heat fluxes is shown in Fig. 5. The β pattern during Rice occurred because of the high values of LE when compared to H . There was greater β variability during Fallow 2 (austral fall and winter) than

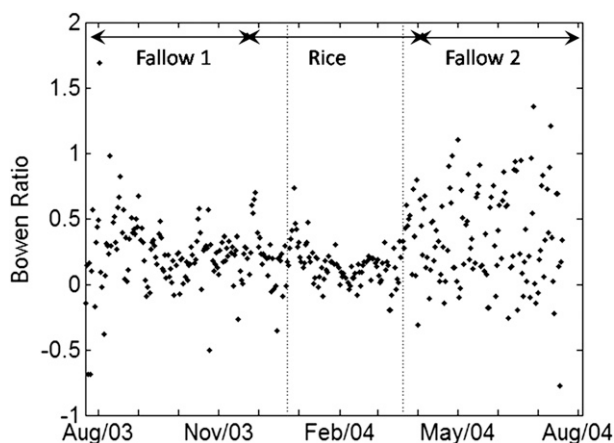


FIG. 5. Seasonal variation of Bowen ratio during the rice-growing and fallow periods for the rice paddy in Paraíso do Sul, Brazil. The vertical dotted lines indicate the flooded period.

during Fallow 1 (austral winter and spring) and a strong decrease as the crop emerged and the canopy fully developed. At the end of the crop-growing season, as the rice crop senesced, β steadily increased. The Bowen ratio averaged over the entire Fallow periods was significantly higher ($\beta = 0.25$) than during the Rice period ($\beta = 0.15$), indicating a greater proportion of R_n being used to warm the atmosphere in the surrounding region. These results for the Rice period agree with previous studies, such as Alberto et al. (2009), who found β values of 0.14 for flooded rice fields and 0.25 for aerobic rice fields, and Tsai et al. (2007), who found 0.16 over a rice paddy in Taiwan, both using the eddy covariance system. According to Suyker and Verma (2008) these trends reflect the well-watered conditions and the control of leaf area on energy partitioning during the crop-growing season.

c. Evapotranspiration

The Bowen ratio was also used to correct LE as a means to generate the experimental ET, as described in section 2c. Annual ET and LAI seasonality is shown in Fig. 6. Evapotranspiration reached almost 7 mm day^{-1} during the Rice period, when the crop was at the end of the reproductive phase (flowering) and LAI was at its peak ($4.57 \text{ m}^2 \text{ m}^{-2}$). During the twelfth week following the planting period, in the beginning of February, LAI reached its highest values. Hatala et al. (2012), using the eddy covariance method in a rice paddy, found daily evaporation up to 10 mm day^{-1} . In northern India, at Dehra Dun, Bhardwaj (1983) carried out experiments with lysimeters and observed a maximum value of ET of 6.5 mm day^{-1} at week 6 after transplanting, which corresponds to week 10 after planting in semiwet conditions. A maximum ET value of 7.2 mm day^{-1} was reported in

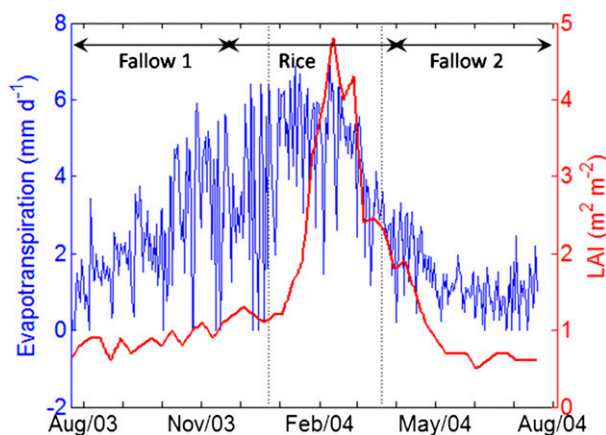


FIG. 6. Daily-mean ET (blue line) and daily LAI (red line) in a rice paddy in Paraíso do Sul, Brazil, from July 2003 to June 2004. The vertical dotted lines represent the flooded period.

semiarid conditions on the Indian subcontinent 9 weeks after rice transplanting (roughly 13 weeks after planting) by Sandhu et al. (1982). More recently, Tyagi et al. (2000), also using lysimeters, reported a maximum ET of 6.61 mm day^{-1} at week 11 after rice transplanting under semiarid conditions in Karmal, India. From week 12 after planting to the end of the rice-growing period (week 19 after planting), a steady decrease in ET from 5.41 to 2.27 mm day^{-1} was observed (Fig. 6). This reduction in ET occurred mainly because of a drastic decrease of LAI due to leaf senescence during crop maturation, when irrigation was no longer performed.

Over the Rice period (132 days), integrated ET was 562 mm. Alberto et al. (2011) obtained the growing rice ET value in the range of 400–556 mm. Tyagi et al. (2000) reported an evapotranspiration of 587 mm during the Rice period, whereas Sandhu et al. (1982) obtained an ET of 701 mm using the water balance approach. These values are 5% and 20% greater than our ET, respectively. Vu et al. (2005) also calculated evapotranspiration in three Rice cultivars from lysimeters for four different experiments in Japan: in the years 1998 and 1999 at Tsukuba and in 2002 and 2003 at Tokyo. The results from Vu et al. (2005) indicate that ET may have considerable variability among different cultivars, depending on plant height, canopy architecture, length of developmental cycle, leaf stomata opening, leaf density, and structure, among other traits that may affect crop evapotranspiration. Furthermore, different accumulative ET was observed for the same cultivar, indicating that interannual variability of climate may also affect ET. Hirasawa (1995) reported that environmental conditions such as vapor pressure deficit, solar radiation, air temperature, and wind speed, among others, affect ET through an influence on water evaporation at the leaf–air interface.

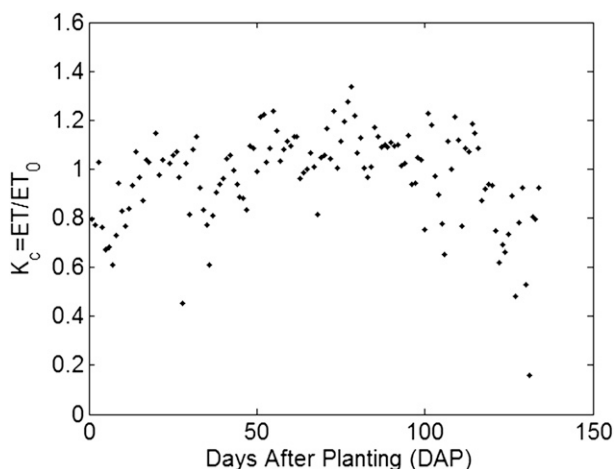


FIG. 7. Daily variation of K_c during the rice-growing period in Paraíso do Sul, Brazil, for the 2003/04 growing season.

During the Fallow 1 and Fallow 2 periods, the accumulated values of ET were 305 and 131 mm, respectively. Adding ET values in both Fallow periods and the Rice period, the total evapotranspiration throughout the year was 998 mm, with each Fallow period contributing 30% and 1.4% to the annual evapotranspiration, respectively. This is very close to the annual ET value found by Hossen et al. (2012) in a year for a double-rice-crop paddy field and around 150 mm lower than that found by Hatala et al. (2012) in a year for a single rice crop.

1) CROP COEFFICIENT

The ET_o from Eq. (10), also used to estimate the crop coefficient, provides average daily evaporation and is widely used in planning and water optimization for irrigated fields. Crop coefficients values varied from 0.6 to 1.3 throughout the growing season (Fig. 7), although during the first 30 days, mean K_c was $0.98 (\pm 0.29)$. Low LAI values (less than 1.0) during the first period resulted in soil evaporation being the major component of ET. As a crop grows and develops, the exposure of the soil surface to the incoming solar radiation decreases and transpiration from leaf area increases, increasing K_c , which, on average, was $1.05 (\pm 0.20)$. As the end of the growing season approaches, decrease in K_c is expected, confirmed by the average $0.99 (\pm 0.18)$ during crop maturation. Results for K_c presented in this study are within the range of the values reported by the FAO for rice and by Alberto et al. (2011).

2) COMPARISON OF ESTIMATES OF EVAPOTRANSPIRATION FROM $K_c ET_o$ AND ET_{PM}

An estimate of evapotranspiration was performed using the Penman–Monteith equation from Eq. (4) with

the aerodynamic and surface resistance estimated through the specific crop height and LAI from remote sensing, as explained in section 2d. The surface resistance in Eq. (9) was the same used in ET_o calculation. Measured ET was then compared against ET_{PM} and an estimation using the reference evapotranspiration (ET_{FAO} ; Fig. 8). During the rice period, $ET_{FAO} = K_c ET_o$, where FAO K_c was used [$K_c = 1.05, 1.2$, and 0.9 for initial, mid-, and end season periods, respectively (Allen et al. 1998)]. During the fallow periods, $ET_{FAO} = ET_o$. For each period analyzed, we compared the slope of the linear fit between experimental (ET) and estimated (ET_{PM} and ET_{FAO}) evapotranspiration rate. In general, ET_{FAO} and ET_{PM} represented the ET well in the Fallow periods. During these periods, the surface cover in the study region was similar to the hypothetical surface that ET_o represents (section 3c), and with no water deficit. During the Rice period, ET_{PM} increased as the crop developed, being more evident after the paddy was flooded, and kept that way onward (data not shown). The integrated values of ET_{PM} and ET_{FAO} (593 and 596 mm, respectively) were very similar and overestimate experimental ET. During the Rice period, the slope of the linear regression between estimated and experimental ET was 0.78 for ET_{PM} and 0.73 for ET_{FAO} . Therefore, using some specific crop parameters like LAI and crop height can be an easy and interesting method to estimate ET in lowland regions. In this particular case, LAI was estimated from satellite data that were easily accessible. Crop height is also not very difficult to describe during the growing season, as modern semidwarf rice cultivars used in southern Brazil do not differ greatly in plant height.

4. Summary and conclusions

Energy and water balance components were analyzed over a paddy rice farm in a subtropical location in southern Brazil. Experimental data were obtained using an eddy covariance system from 22 July 2003 to 21 July 2004 (366 days), comprising three distinct periods with respect to soil use: Fallow 1, Rice, and Fallow 2. From late December through mid-March, within the Rice period, the soil was covered (flooded) by a 5–10-cm water layer.

As presented in previous studies using eddy covariance measurements, the results over the entire experiment period show that net radiation could not be only explained by sensible, latent, and soil heat fluxes. The percentage of residual energy with respect to the total available energy (R_n) is associated with the amount of soil water content, varying from 10% during the drier Fallow period to up to 20% during the flooded period, indicating that the remaining energy was stored in the canopy. The majority of R_n was explained by the latent

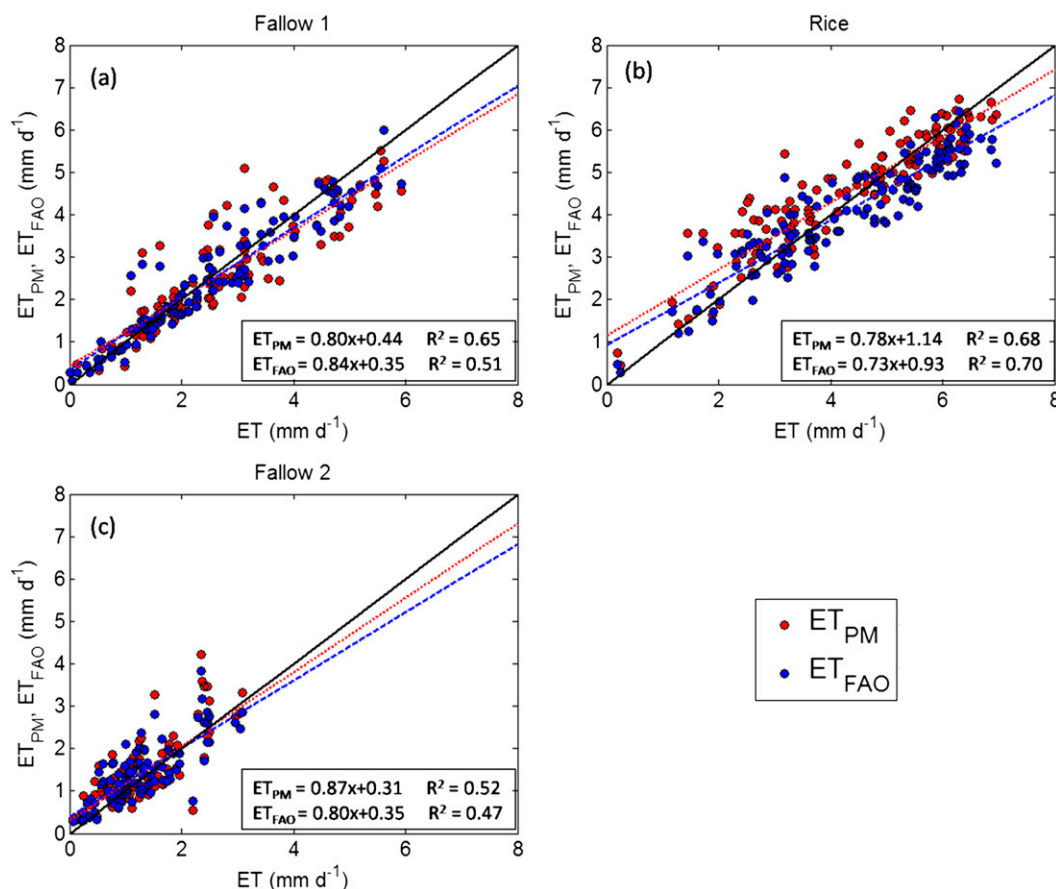


FIG. 8. Scatterplots of measured and estimated ET for (a) Fallow 1, (b) Rice, and (c) Fallow 2 in Paraíso do Sul, Brazil. The dashed (blue) and dotted (red) lines represent the linear fit of the data for ET_{FAO} and ET_{PM} , respectively; the solid black line is the 1:1 line.

heat flux (68%, 64%, and $\approx 95\%$ for Fallow 1, Rice, and Fallow 2 periods, respectively), whereas the sensible heat flux remained almost constant during the entire period. Consequently, the Bowen ratio variability was mostly explained by the variations in the LE, in particular during the Rice period, when it exceeded H in almost one order of magnitude. During Fallow 1 and Fallow 2, the Bowen ratio was approximately 0.25, whereas during Rice it did not exceed 0.15, indicating that the majority of the net radiation was converted into latent heat flux.

As a complementary source of information, environmental measurements (i.e., meteorological forcing such as air temperature, wind speed, relative humidity, surface pressure, etc.) were used to corroborate the relationship between eddy covariance and plant measurements. For instance, over the study region, the atmosphere with low water demand for plant transpiration or soil evaporation resulted in VPD values lower than 1 kPa during most of the days. Furthermore, rice paddies are usually embedded in a larger area of lowlands within a river basin, creating a microclimate with a large amount of water

available for ET, which increases the atmospheric specific humidity (and consequently, relative humidity) near the surface. However, variables such as relative humidity have to be used with care, in particular when averaged over the day since it could result in high bias because of the nighttime values. For future work, it is suggested to assess the statistics computation for the atmospheric variables and how the results could be affected by data uncertainty.

Crop coefficients for flooded rice grown in subtropical regions are not available by the FAO. Therefore, this study lays groundwork for crop coefficient estimation over a subtropical lowland flooded paddy rice. Nonetheless, the crop coefficient values found during the rice-growing period are within the ranges reported by FAO for tropical regions.

Estimates of evapotranspiration using the reference ET and the Penman–Monteith equation (ET_{PM}), with aerodynamic and surface resistance estimated using specific crop height (z_o) and LAI from remote sensing, showed similar results during the Fallow periods. It

suggests that these similarities result from the site location, in a lowland zone where, in general, soil water content is high and there is virtually no water deficit. During the Rice period, ET_{PM} yielded better results, suggesting that the use of specific crop parameters is a viable alternative for ET estimation over vegetated lowland regions.

Acknowledgments. The authors acknowledge the National Council for Scientific and Technological Development (CNPq, Brazil), the Coordination for the Improvement of Higher Education Personnel (CAPES, Brazil), the Foundation for Research of Rio Grande do Sul State (FAPERGS), and NASA for the project “Integrating NASA Earth Sciences Research Results into Decision Support Systems for Agriculture and Water Management in South America” (Grant NNNH08ZDA001N-DECISIONS) for their financial support.

REFERENCES

- Acevedo, O. C., O. L. L. Moraes, G. A. Degrazia, and L. E. Medeiros, 2006: Intermittency and the exchange of scalars in the nocturnal surface layer. *Bound.-Layer Meteor.*, **119**, 41–55, doi:10.1007/s10546-005-9019-3.
- , —, —, D. R. Fitzjarrald, A. O. Manzi, and J. G. Campos, 2009: Is friction velocity the most appropriate scale for correcting nocturnal carbon dioxide fluxes? *Agric. For. Meteor.*, **149**, 1–10, doi:10.1016/j.agrformet.2008.06.014.
- Alberto, Ma. C. R., R. Wassmann, T. Hirano, A. Miyata, A. Kumar, A. Padre, and M. Amante, 2009: CO_2 /heat fluxes in rice fields: Comparative assessment of flooded and non-flooded in the Philippines. *Agric. For. Meteor.*, **149**, 1737–1750, doi:10.1016/j.agrformet.2009.06.003.
- , —, —, —, R. Hatano, A. Kumar, A. Padre, and M. Amante, 2011: Comparisons of energy balance and evapotranspiration between flooded and aerobic rice fields in the Philippines. *Agric. Water Manage.*, **98**, 1417–1430, doi:10.1016/j.agwat.2011.04.011.
- Allen, R. G., L. S. Pereira, D. Raes, and M. Smith, 1998: Crop evapotranspiration: Guidelines for computing crop water requirements. FAO Irrigation and Drainage Paper 56, 300 pp. [Available online at www.fao.org/docrep/X0490E/X0490E00.htm.]
- Aubinet, M., and Coauthors, 2000: Estimates of the annual net carbon and water exchange of forests: The EUROFLUX methodology. *Adv. Ecol. Res.*, **30**, 113–175, doi:10.1016/S0065-2504(08)60018-5.
- Baldocchi, D. D., B. B. Hicks, and T. P. Meyers, 1988: Measuring biosphere–atmosphere exchanges of biologically related gases with micrometeorological methods. *Ecology*, **69**, 1331–1340, doi:10.2307/1941631.
- Bethune, M., N. Austin, and S. Maher, 2001: Qualifying the water budget of irrigated rice in the Shepparton irrigation region, Australia. *Irrig. Sci.*, **20**, 99–105, doi:10.1007/s002710100035.
- Bhardwaj, S. P., 1983: Study on consumptive use rates in weighing type lysimeters for irrigation. Central Soil and Water Conservation Research Institute Rep., 100 pp.
- Cava, D., D. Contini, A. Donato, and P. Martano, 2008: Analysis of short-term closure of the surface energy balance above short vegetation. *Agric. For. Meteor.*, **148**, 82–93, doi:10.1016/j.agrformet.2007.09.003.
- Conab, cited 2013: The National Supply Company, Ministry of Agriculture, Livestock and Supply. [Available online at <http://www.conab.gov.br/conteudos.php?a=1252&t=->.]
- de Medeiros, G. A., F. B. Arruda, and E. Sakai, 2005: Crop coefficient for irrigated beans derived using three reference evaporation methods. *Agric. For. Meteor.*, **135**, 135–143, doi:10.1016/j.agrformet.2005.11.010.
- Ek, M. B., K. E. Mitchell, Y. Lin, E. Rogers, P. Grunmann, V. Koren, G. Gayno, and J. D. Tarpley, 2003: Implementation of Noah land surface model advances in the National Centers for Environmental Prediction operational mesoscale Eta model. *J. Geophys. Res.*, **108**, 8851, doi:10.1029/2002JD003296.
- Foley, J. A., I. C. Prentice, N. Ramankutty, S. Levis, D. Pollard, S. Sitch, and A. Haxeltine, 1996: An integrated biosphere model of land surface processes, terrestrial carbon balance and vegetation dynamics. *Global Biogeochem. Cycles*, **10**, 603–628, doi:10.1029/96GB02692.
- Grismer, M. E., M. Orang, R. Snyder, and R. Matyac, 2002: Pan evaporation to reference evapotranspiration conversion methods. *J. Irrig. Drain. Eng.*, **128**, 180–184, doi:10.1061/(ASCE)0733-9437(2002)128:3(180).
- Hatala, J. A., M. Detto, O. Sonnentag, S. J. Deverel, J. Verfaillie, and D. D. Baldocchi, 2012: Greenhouse gas (CO_2 , CH_4 , H_2O) fluxes from drained and flooded agricultural peatlands in the Sacramento–San Joaquin Delta. *Agric. Ecosyst. Environ.*, **150**, 1–18, doi:10.1016/j.agee.2012.01.009.
- Hernandez-Ramirez, G., J. L. Hatfield, J. H. Prueger, and T. J. Sauer, 2010: Energy balance and turbulent flux partitioning in a corn–soybean rotation in the Midwestern US. *Theor. Appl. Climatol.*, **100**, 79–92, doi:10.1007/s00704-009-0169-y.
- Hirasawa, T., 1995: Water relations in plants. *Physiology*, T. Matsuo et al., Eds., Vol. 2, *Science of the Rice Plant*, Food and Agriculture Policy Research Center, 434–460.
- Hossen, Md. S., M. Mano, M. Miyata, Md. A. Baten, and T. Hiyama, 2012: Surface energy partitioning and evapotranspiration over a double-cropping paddy field in Bangladesh. *Hydrol. Processes*, **26**, 1311–1320, doi:10.1002/hyp.8232.
- Kanda, M., A. Inagaki, M. O. Letzel, S. Raasch, and T. Watanabe, 2004: LES study of the energy imbalance problem with eddy covariance fluxes. *Bound.-Layer Meteor.*, **110**, 381–404, doi:10.1023/B:BOUN.0000007225.45548.7a.
- Kanemasu, E. T., and Coauthors, 1992: Surface flux measurements in FIFE: An overview. *J. Geophys. Res.*, **97**, 18 547–18 555, doi:10.1029/92JD00254.
- Kiniry, J. R., J. A. Landivar, M. Witt, T. J. Gerik, J. Cavero, and L. J. Wade, 1998: Radiation-use efficiency response to vapor pressure deficit for maize and sorghum. *Field Crops Res.*, **56**, 265–270, doi:10.1016/S0378-4290(97)00092-0.
- Kucharik, C. J., and T. E. Twine, 2007: Residue, respiration, and residuals: Evaluation of a dynamic agroecosystem model using eddy flux measurements and biometric data. *Agric. For. Meteor.*, **146**, 134–158, doi:10.1016/j.agrformet.2007.05.011.
- Lage, M., A. Bamouh, M. Karrou, and M. Mourid, 2003: Estimation of rice evapotranspiration using microlysimeter technique and comparison with FAO Penman–Monteith and Pan evaporation methods under Moroccan condition. *Agronomie*, **23**, 625–631, doi:10.1051/agro:2003040.

- Lecina, S., A. Martinez-Cob, P. J. Perez, F. J. Villalobos, and J. J. Baselga, 2003: Fixed versus variable bulk canopy resistance for reference evapotranspiration estimation using the Penman–Monteith equation under semiarid condition. *Agric. Water Manage.*, **60**, 181–198, doi:[10.1016/S0378-3774\(02\)00174-9](https://doi.org/10.1016/S0378-3774(02)00174-9).
- Leuning, R., E. van Gorsel, W. J. Massman, and P. R. Isaac, 2012: Reflections on the surface energy imbalance problem. *Agric. For. Meteorol.*, **156**, 65–74, doi:[10.1016/j.agrformet.2011.12.002](https://doi.org/10.1016/j.agrformet.2011.12.002).
- Maruyama, A., and T. Kuwagata, 2010: Coupling land surface and crop growth models to estimate the effects of changes in the growing season on energy balance and water use of rice paddies. *Agric. For. Meteorol.*, **150**, 919–930, doi:[10.1016/j.agrformet.2010.02.011](https://doi.org/10.1016/j.agrformet.2010.02.011).
- Noilhan, J., and S. Planton, 1989: A simple parameterization of land surface processes for meteorological models. *Mon. Wea. Rev.*, **117**, 536–549, doi:[10.1175/1520-0493\(1989\)117<0536:ASPOLS>2.0.CO;2](https://doi.org/10.1175/1520-0493(1989)117<0536:ASPOLS>2.0.CO;2).
- Oke, T. R., 1987: *Boundary Layer Climates*. 2nd ed. Methuen, 435 pp.
- Sakai, R. K., D. R. Fitzjarrald, and K. E. Moore, 2001: Importance of low-frequency contributions to eddy fluxes observed over rough surfaces. *J. Appl. Meteorol.*, **40**, 2178–2192, doi:[10.1175/1520-0450\(2001\)040<2178:IOLFCT>2.0.CO;2](https://doi.org/10.1175/1520-0450(2001)040<2178:IOLFCT>2.0.CO;2).
- Sandhu, B. S., K. L. Khera, and B. Singh, 1982: A note on the use of irrigation water and yield of transplanted rice in relation to time of last irrigation. *Indian J. Agric. Sci.*, **52**, 870–872.
- Shah, S. B., and R. J. Edling, 2000: Daily evapotranspiration prediction from Louisiana flooded rice field. *J. Irrig. Drain. Eng.*, **126**, 8–13, doi:[10.1061/\(ASCE\)0733-9437\(2000\)126:1\(8\)](https://doi.org/10.1061/(ASCE)0733-9437(2000)126:1(8)).
- Soil Survey Staff, 1999: *Soil Taxonomy: A Basic System of Soil Classification for Making and Interpreting Soil Surveys*. Agriculture Handbook, No. 436, USDA, 871 pp. [Available online at www.nrcs.usda.gov/Internet/FSE_DOCUMENTS/nrcs142p2_051232.pdf.]
- Streck, N. A., I. Lago, F. B. Oliveira, A. B. Heldwein, L. A. Avila, and L. C. Bosco, 2011: Modeling the development of cultivated rice and weedy red rice. *Trans. ASABE*, **54**, 371–384, doi:[10.13031/2013.36234](https://doi.org/10.13031/2013.36234).
- Suyker, A. E., and S. B. Verma, 2008: Interannual water vapor and energy exchange in an irrigated maize-based agroecosystem. *Agric. For. Meteorol.*, **148**, 417–427, doi:[10.1016/j.agrformet.2007.10.005](https://doi.org/10.1016/j.agrformet.2007.10.005).
- Tsai, J. L., B. J. Tsuang, P. S. Lu, M. H. Yao, and Y. Shen, 2007: Surface energy components and land characteristics of a rice paddy. *J. Appl. Meteor. Climatol.*, **46**, 1879–1900, doi:[10.1175/2007JAMC1568.1](https://doi.org/10.1175/2007JAMC1568.1).
- Tsvang, L. R., M. M. Fedorov, B. A. Kader, S. L. Zubkovskii, T. Foken, S. H. Richter, and Ya. Zeleny, 1991: Turbulent exchange over a surface with chessboard-type inhomogeneities. *Bound.-Layer Meteorol.*, **55**, 141–160, doi:[10.1007/BF00119331](https://doi.org/10.1007/BF00119331).
- Tyagi, N. K., D. K. Sharma, and S. K. Luthra, 2000: Determination of evapotranspiration and crop coefficient of rice and sunflower with lysimeters. *Agric. Water Manage.*, **45**, 41–64, doi:[10.1016/S0378-3774\(99\)00071-2](https://doi.org/10.1016/S0378-3774(99)00071-2).
- Vu, S. H., H. Watanabe, and K. Takagi, 2005: Application of FAO-56 for evaluating evapotranspiration in simulation of pollutant runoff from paddy rice field in Japan. *Agric. Water Manage.*, **76**, 195–210, doi:[10.1016/j.agwat.2005.01.012](https://doi.org/10.1016/j.agwat.2005.01.012).
- Walko, R. L., and Coauthors, 2000: Coupled atmosphere–biophysics–hydrology models for environmental modeling. *J. Appl. Meteorol.*, **39**, 931–944, doi:[10.1175/1520-0450\(2000\)039<0931:CABHMF>2.0.CO;2](https://doi.org/10.1175/1520-0450(2000)039<0931:CABHMF>2.0.CO;2).
- Wilson, K. B., and D. D. Baldocchi, 2000: Seasonal and interannual variability of energy fluxes over a broadleaved temperate deciduous forest in North America. *Agric. For. Meteorol.*, **100**, 1–18, doi:[10.1016/S0168-1923\(99\)00088-X](https://doi.org/10.1016/S0168-1923(99)00088-X).
- , and Coauthors, 2002: Energy balance closure at FLUXNET sites. *Agric. For. Meteorol.*, **113**, 223–243, doi:[10.1016/S0168-1923\(02\)00109-0](https://doi.org/10.1016/S0168-1923(02)00109-0).
- Wyngaard, J. C., 1990: Scalar fluxes in the planetary boundary layer—Theory, modeling, and measurement. *Bound.-Layer Meteorol.*, **50**, 49–75, doi:[10.1007/BF00120518](https://doi.org/10.1007/BF00120518).

Copyright of Journal of Hydrometeorology is the property of American Meteorological Society and its content may not be copied or emailed to multiple sites or posted to a listserv without the copyright holder's express written permission. However, users may print, download, or email articles for individual use.